

OMAE2017-61175

FREE-SURFACE FLOW SIMULATIONS WITH INTERACTIVELY MOVING BODIES

Arthur E.P. Veldman*
Henk Seubers
Peter van der Plas

Institute for Mathematics and Computer Science
University of Groningen
P.O. Box 407, 9700 AK Groningen
The Netherlands
{a.e.p.veldman, h.seubers, p.van.der.plas}@rug.nl

Joop Helder

MARIN
P.O. Box 28, 6700 AA Wageningen
The Netherlands
j.helder@marin.nl

ABSTRACT

The simulation of free-surface flow around moored or floating objects faces a series of challenges, concerning the flow modelling and the numerical solution method. One of the challenges is the simulation of objects whose dynamics is determined by a two-way interaction with the incoming waves. The 'traditional' way of numerically coupling the flow dynamics with the dynamics of a floating object becomes unstable (or requires severe underrelaxation) when the added mass is larger than the mass of the object. To deal with this two-way interaction, a more simultaneous type of numerical coupling is being developed. The paper will focus on this issue. To demonstrate the quasi-simultaneous method, a number of simulation results for engineering applications from the offshore industry will be presented, such as the motion of a moored TLP platform in extreme waves, and a free-fall life boat dropping into wavy water.

1 INTRODUCTION

Over the centuries, understanding the motion and behavior of waves in nature has been a very popular subject among researchers from various fields of science. Even today, when we have highly capable numerical methods and computational power at our disposal, numerical modeling of water wave propagation remains a formidable challenge. During the development

of the ComFLOW simulation method [1–5] many of the numerical challenges have been tackled:

- Waves should be allowed to freely enter or leave the domain, requiring absorbing or non-reflecting boundary conditions which are able to deal with the dispersive character of waves on deep water [6]. Also attention has to be paid to an accurate description of wave propagation (reconstruction and advection). More info on these aspects is to be found in the PhD thesis of Duz [7] and the forthcoming papers [8,9].
- The turbulence model not only has to deal with coarse grids, but should also recognize wall-bounded turbulence from free-surface turbulence. This is tackled with a new class of adaptive, minimum-dissipation turbulence LES models [10–12]
- The numerical coupling of the flow dynamics with the dynamics of a floating object has to deal with situations where the added mass is larger than the mass of the object. Hereto a more simultaneous type of numerical coupling is being developed. This paper contains more details about this issue.
- The efficiency of the simulations is enhanced by means of local grid refinement and parallelisation [13, 14].

When the objects (or structures) under study are moving, either free-floating or attached to a mooring system, the interaction between the incoming waves and the dynamics of the structure comes into play. Physically, we can distinguish one-way or two-

*Address all correspondence to this author.

way interaction. In the former case the structure ‘simply’ reacts to the oncoming flow field. But in the latter case the interaction is such that the motion of the structure influences the flow field around the structure. The latter case also poses most challenges to the numerical coupling between flow and structure.

Such a numerical coupling approach can be *aggregated* (monolithic) or *segregated* (partitioned). In the former case all discrete equations of motion are combined into one single set of equations which is then solved simultaneously. In the latter case two separate discrete systems (modules) can be recognized equipped with recipes to exchange information between the two separate modules. On the one hand this enhances the flexibility (modularity) of the approach, but on the other hand it requires a (hierarchical) iterative exchange of information between the modules with its consequences for numerical stability and convergence. Below we describe our efforts to find a compromise between the robust monolithic approach and the more flexible, but vulnerable, partitioned approach. We will see that the ratio between the mass of the structure and its added fluid mass plays an essential role.

The organization of the paper is as follows. After an introduction of the flow equations, the numerical coupling strategy between fluid and solid structure is studied. The paper finishes with some practical applications: a falling lifeboat and a moored TLP platform. Some of these applications are validated by experiments carried out at MARIN.



FIGURE 1. DROP TEST WITH FREE-FALL LIFEBOAT (FROM: WWW.VERHOEF.EU)

2 MATHEMATICAL FLOW MODEL

Incompressible, turbulent fluid flow can be modelled by means of the Navier–Stokes equations.

$$\mathcal{M}\mathbf{u} = 0, \quad \frac{\partial \mathbf{u}}{\partial t} + \mathcal{C}(\mathbf{u})\mathbf{u} + \mathcal{G}p - \mathcal{V}\mathbf{u} = \mathbf{f}. \quad (1)$$

Here \mathcal{M} is the divergence operator, which describes conservation of mass. Conservation of momentum is based on the convection operator $\mathcal{C}(\mathbf{u})\mathbf{v} \equiv \nabla(\mathbf{u} \otimes \mathbf{v})$, the pressure gradient operator $\mathcal{G} = \nabla$, the viscous diffusion operator $\mathcal{V}(\mathbf{u}) \equiv \nabla \cdot \nu \nabla \mathbf{u}$ and a forcing term \mathbf{f} . The kinematic viscosity is denoted by ν .

Turbulence is modelled by means of large-eddy simulation (LES) using a low-dissipation QR-model as formulated by Verstappen [10]. For its use in maritime applications, see [15, 16]. This model has been refined and extended in the PhD thesis of Rozema [11, 12] and is now in use e.g. at the Center for Turbulent Research (Stanford University) [17].

The Navier–Stokes equations (1) are discretized on an Arakawa C-grid. The second-order finite-volume discretization of the continuity equation at the ‘new’ time level $^{n+1}$ is given by

$$M^0 \mathbf{u}^{n+1} = -M^\Gamma \mathbf{u}_\Gamma^{n+1}, \quad (2)$$

where M^0 acts on the interior of the domain and M^Γ acts on the boundaries of the domain (with \mathbf{u}_Γ denoting the velocity at the boundary). In the discretized momentum equation, convection $C(\mathbf{u}_h)$ and diffusion D are discretized explicitly in time. The pressure gradient is discretized at the new time level. In this exposition, for simplicity reasons the first-order forward Euler time integration will be used. In the actual calculations, a second-order Adams–Bashforth method is being applied.

Letting the diagonal matrix Ω denote the matrix containing the geometric size of the control volumes, gives the discretized momentum equation as

$$\Omega \frac{\mathbf{u}^{n+1} - \mathbf{u}^n}{\delta t} = -C(\mathbf{u}^n) \mathbf{u}^n + \mathbf{V} \mathbf{u}^n - G p^{n+1} + \mathbf{f}. \quad (3)$$

For divergence-free velocity fields \mathbf{u} , the conservative discrete convection operator is skew-symmetric, such that convection does not contribute to energy production or dissipation; see Verstappen and Veldman [18]. In particular, its discretization preserves the energy of the flow and does not produce artificial diffusion. To make the discretization fully energy-preserving, the discrete gradient operator and the divergence operator are each other’s negative transpose, i.e. $G = -M^{0T}$, thus mimicking the analytic symmetry $\nabla = -(\nabla \cdot)^T$. In this way, also the work done by the pressure vanishes discretely.

The solution of the discrete Navier–Stokes equations is split into two steps. Firstly, an auxiliary variable $\tilde{\mathbf{u}}$ is defined through

$$\Omega \frac{\tilde{\mathbf{u}} - \mathbf{u}^n}{\delta t} = -C(\mathbf{u}^n) \mathbf{u}^n + D\mathbf{u}^n + \mathbf{f}. \quad (4)$$

With this abbreviation, the discrete momentum equation (3) can be reformulated as

$$\mathbf{u}^{n+1} = \tilde{\mathbf{u}} - \delta t \Omega^{-1} G p^{n+1}. \quad (5)$$

Secondly, by imposing discrete mass conservation (2) at the new time level, substitution of (5) results in a discrete Poisson equation for the pressure:

$$\delta t M^0 \Omega^{-1} G p^{n+1} = M^0 \tilde{\mathbf{u}} + M^\Gamma \mathbf{u}^{n+1}. \quad (6)$$

Sometimes, this step is geometrically interpreted as a projection step. Unfortunately this phrasing creates a negative association sounding as a correction for something that needs to be repaired, but here this step is just a straightforward reformulation of the original discrete equations (2) and (3).

The liquid region and the free liquid surface are described by an improved VOF-method; see e.g. Hirt and Nichols [19], Kleefsman et al. [1] and Düz [7].

3 FLUID–SOLID BODY COUPLING

A further step is to allow the moving object to interact with the fluid dynamics, e.g. it is floating on the water surface. This physical two-way coupling has to be mirrored in the numerical coupling algorithm between the flow solver and the solid-body solver. The coupling takes place along the common interface Γ between the fluid and the solid body; quantities involved are the dynamics (position and acceleration) of the solid body, and the dynamics of the fluid (in particular its pressure loads); see Fig. 2.

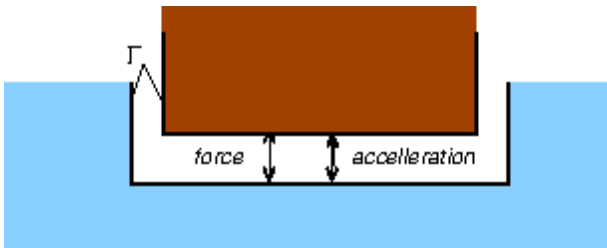


FIGURE 2. SCHEMATIC PARTITIONING BETWEEN FLUID AND SOLID BODY, WITH INFORMATION EXCHANGE ALONG THEIR COMMON INTERFACE Γ .

1. The *coupling conditions* at the interface between fluid and solid body basically express ‘continuity’ of the physics on both sides of the common interface Γ . The *kinematic* condition expresses that the boundary of the liquid region (partially) coincides with the surface of the solid body. In particular, material particles on both sides have the same velocity and acceleration (when the no-slip condition does not hold, only the normal component is continuous). Hence, it makes sense to talk about the velocity at the interface \mathbf{u}_Γ . Additionally, the *dynamic* coupling condition is based on Newton’s 3rd law “*action = –reaction*”, which expresses equilibrium of forces. In particular, we denote the fluid pressure by p_Γ . In the sequel, we will formulate the coupled problem in terms of the two interface variables: \mathbf{u}_Γ and p_Γ .
2. The *solid-body dynamics* is governed by an equation describing the acceleration $\dot{\mathbf{u}}$ of the solid body when reacting to the forces and moments \mathbf{f} exerted by the fluid. The latter are found by integration of the liquid pressure and the viscous stresses over the common interface Γ . In abstract terms we denote this relation by

$$\text{solid body dynamics: } \dot{\mathbf{u}}_\Gamma = D p_\Gamma. \quad (7)$$

The dynamics operator D involves the integration of the fluid pressure and the viscous stresses over the interface to obtain the force and moments acting on the body. Through the dynamics equations of the solid body these lead to an acceleration of the body. Thus the eigenvalues of D are inversely related to the body mass and its moments of inertia. Note that we do not show eventual external forces, as they play no essential role in the coupling algorithm.

3. The *fluid dynamics* governs the reaction of the fluid to the motion of the solid body. The latter creates a boundary condition along the interface Γ which has to be added to the Navier–Stokes equations (1). As a result, the pressure along the interface and acting on the solid body can be computed. In abstract notation we write

$$\text{fluid dynamics: } p_\Gamma = -M_a \dot{\mathbf{u}}_\Gamma, \quad (8)$$

where M_a is related to the so-called *added mass* operator (in the notation we ignore the integration of the pressure to yield a force). Again, terms in \mathbf{u} have been omitted because of their minor role in the analysis of the coupling process.

The above formulation (7)+(8) in principle shows two equations for the two unknowns along the interface: pressure and acceleration. Their coupling can be done in an *aggregated / monolithic* or *segregated / partitioned* way. An aggregated (or strong) coupling recombines both equations (or modules) into one single global system which is solved simultaneously. In contrast, a

segregated (or weak) coupling keeps the two equations apart and solves them in an iterative way. The former approach may not always be possible, e.g. due to their ‘black-box’ character, or due to the large complexity of the modules; the latter approach may diverge.

3.1 Weak coupling

In practice often a segregated approach is followed. The usual way is to let the fluid determine a pressure field p_Γ^{old} which, together with the visous stresses, moves the solid body:

$$\dot{\mathbf{u}}_\Gamma^{\text{new}} = Dp_\Gamma^{\text{old}}. \quad (9)$$

This motion of the solid body is then transferred to the fluid to react with a new pressure field:

$$p_\Gamma^{\text{new}} = -M_a \dot{\mathbf{u}}_\Gamma^{\text{new}}. \quad (10)$$

In this way, we effectively have created an iterative process

$$p_\Gamma^{\text{new}} = -M_a D p_\Gamma^{\text{old}}. \quad (11)$$

The iterations in such a weak coupling method will converge if and only if the spectral radius of the iteration matrix $\rho(M_a D) < 1$. Recalling that D inversely scales with the mass and inertia of the solid body, this condition becomes a requirement for the ratio between added mass and body mass. Roughly speaking, the solid body should be heavy enough. If it is not, underrelaxation can help achieving convergence, but this will require (many) additional (sub)iterations and diminishes efficiency.

In practice, such iterations can be implemented as follows in the solution process for the Navier–Stokes equation (3) during the time step from $n \rightarrow n + 1$. An additional subiteration process (with iteration count k) is included:

$$\text{solid-body dynamics: } (\dot{\mathbf{u}}_\Gamma^{n+1})^k = D(p_\Gamma^{n+1})^k; \quad (12)$$

$$\text{Navier–Stokes: } (p_\Gamma^{n+1})^{k+1} = M_a (\dot{\mathbf{u}}_\Gamma^{n+1})^k. \quad (13)$$

If necessary, these subiterations can be made convergent by applying (severe) underrelaxation without disturbing the time accuracy of the time integration method, but often at a considerable computational price.

Below we will demonstrate with an example of a falling life boat how many subiterations can be required. Because of this inefficiency, we would like to apply an aggregated approach (which does not require subiterations), or at least to be as close as possible to such an approach. Our favorite example is the quasi-simultaneous method, originally (in the late 1970s) developed for interacting aerodynamic boundary layers along airplane wings [20]; a historic overview is provided in [21, 22].

3.2 Quasi-simultaneous coupling

For iterative efficiency reasons, we would like to follow the monolithic, simultaneous approach as much as possible. If possible, this would be the most efficient numerical coupling; see e.g. Drela [23] for a monolithic implementation of boundary-layer interaction as compared to the partitioned implementation of Veldman [20]. Alas, such a monolithic approach requires access to the internal numerics of the two solvers that are being coupled. In practice, using commercial software, this is often not possible because of the black-box character.

In the current situation, however, the source code of the fluid-flow solver is at our disposal. Then, from a software-engineering point of view, we are able to integrate a simplified version of the solid-dynamics solver into the algorithmic heart of the flow solver. A similar action, but with flow solver and solid-dynamics solver interchanged, makes use of a sophisticated guess for the added mass of the fluid which is integrated with the solid-body dynamics. One step further, applicable when the source code of none of the modules is accessible, is black-box coupling as introduced by Vierendeels and colleagues [24, 25]; see also contributions to the ECCOMAS conference series Coupled Problems, e.g. [26]. A general survey of opportunities and challenges in multi-physics coupling is provided by Keyes et al. [27].

Thus, with the full dynamics operator D being too complex, we look for a good approximation \tilde{D} which anticipates the reaction of the full dynamics D and which is simple enough to be used as a boundary condition inside the Navier–Stokes solver (1). Such an approximation has been proposed in the late 1970s (in a somewhat different context) and was then termed an *interaction law* [20–22] (in modern language it would be called a reduced-order model [24])

$$\dot{\mathbf{u}}_\Gamma = \tilde{D} p_\Gamma. \quad (14)$$

The interaction law (14) is then incorporated in the time integration process in defect formulation:

$$\text{interaction law: } \dot{\mathbf{u}}_\Gamma^{n+1} - \tilde{D} p_\Gamma^{n+1} = (D - \tilde{D}) p_\Gamma^n \quad (15)$$

$$\text{Navier–Stokes: } p_\Gamma^{n+1} - M_a \dot{\mathbf{u}}_\Gamma^{n+1} = 0. \quad (16)$$

Another interpretation in terms of time integration is that the part \tilde{D} of the dynamics equation (7) is treated implicitly and the remaining part $D - \tilde{D}$ explicitly. Note that the viscous stresses need not be part of the interaction law, as they can be handled in a weak fashion.

The interaction law is a boundary condition for the Navier–Stokes equations along the interface Γ . More precisely, it will be implemented as a boundary condition for the pressure Poisson

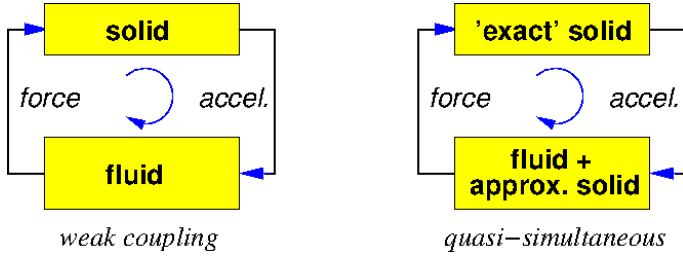


FIGURE 3. WEAK VERSUS QUASI-SIMULTANEOUS COUPLING.

equation (6). The latter is derived by first rewriting the boundary condition (15) for \mathbf{u} as

$$\mathbf{u}_\Gamma^{n+1} - \delta t \tilde{D} p_\Gamma^{n+1} = \mathbf{u}_\Gamma^n + \delta t (D - \tilde{D}) p_\Gamma^n.$$

Then the discrete momentum equation is written in the form (2), wherein the above relation is substituted through the term $M^\Gamma \mathbf{u}_\Gamma$. Finally a relation is obtained featuring p_Γ as a boundary condition for the Poisson equation; see also [28].

The above *quasi-simultaneous* integration can be analysed by eliminating $\tilde{\mathbf{u}}$ from (15)+(16), which leads to

$$(I + M_a \tilde{D}) p_\Gamma^{n+1} = -M_a (D - \tilde{D}) p_\Gamma^n. \quad (17)$$

For $\tilde{D} \equiv 0$, we recover the iteration process (11) which breaks down when M_a is ‘too large’. But with the term $M_a \tilde{D}$ on the left-hand side and the difference $D - \tilde{D}$ on the right-hand side, it will be clear that this process will converge when \tilde{D} is sufficiently close to D , in spite of a possibly ‘large’ M_a .

4 Examples

To show the performance of the quasi-simultaneous approach, two test cases are presented: i) a life boat falling into a breaking wave; and ii) a moored TLP platform.

4.1 Falling life boat

The first test case is a simulation of a life boat dropped into a breaking wave. The life boat has an average density of 320 kg/m^3 , the water a density of 1025 kg/m^3 . It is dropped from 37 m height and hits the water at $t = 2.5 \text{ s}$. A snapshot of the simulations is shown in Fig. 4. The dynamics of the life boat is modelled by means of a 6-DOF mechanical model.

The fluid flow is modelled with the Navier-Stokes equations and solved on a grid consisting of about 0.7 million active (i.e. within the fluid) grid points, with local grid refinement [13, 14] around the life boat (Fig. 4).

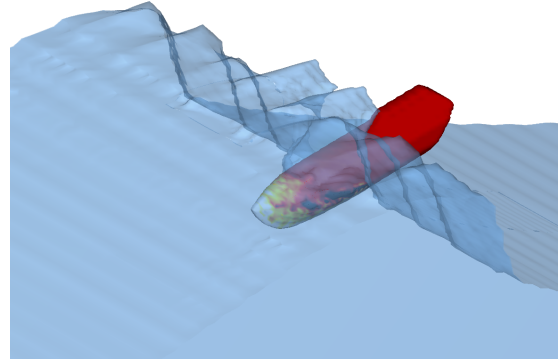


FIGURE 4. A SIMULATION SNAPSHOT OF THE LIFE BOAT FALLING INTO A LARGE WAVE.

For physical accuracy this grid is rather coarse, as the focus in these simulations is on the numerical behaviour of the coupling process. Thus both the weak coupling procedure (11) as well as the quasi-simultaneous procedure (16) have been applied. In the latter case, the interaction law is based on the under-water part of the lifeboat (as the Poisson equation is only solved under water).

The most important result concerns the amount of work that is needed per time step to achieve the coupling between solid-body dynamics and fluid flow. The weak method often requires dozens of subiterations, in each of which a Poisson equation has to be solved. This number is dependent on the amount of fluid that is moved aside by the moving body, represented by the added-mass operator M_a . Fortunately, the later subiterations have a good initial guess so they are not as expensive as the earlier ones. Thus the amount of work is better represented by the total number of SOR-iterations [29] that is needed for all Poisson solves within one time step.

This amount of work is shown in Fig. 5(top). The relation with the added mass becomes visible when plotting the time history of the estimated added mass in Fig. 5(bottom). Note that the ‘gaps’ in the curve are due to a loss of significant digits during the post-processing to obtain a numerical estimation of the added mass. Comparison with Fig. 5(top) shows clearly that the number of iterations grows rapidly when the ‘added-mass ratio’ $\rho(DM_a)$ grows beyond 1. In contrast, the quasi-simultaneous method requires 1 or 2 subiterations (with additional Poisson solver), resulting in much less work per time step (Fig. 5). This reduction in the number of subiterations is highly independent of the grid size and of the chosen Poisson solver. More specifically, the number of subiterations is (to first order) only dependent on the difference between the analytic pendants of D and \tilde{D} .

The added mass varies greatly over time during the impact, as the boat enters the water and a larger part of the wave has to respond. It is clear that the relaxation-based method (12)+(13)

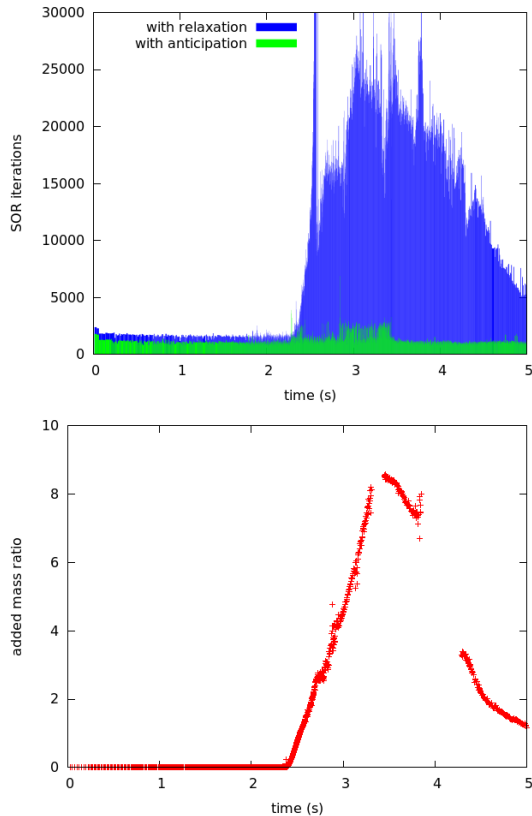


FIGURE 5. *TOP:* THE NUMBER OF SOR ITERATIONS PER TIME STEP FOR THE UNDERRELAXED WEAK COUPLING METHOD (BLUE) AND THE ANTICIPATORY QUASI-SIMULTANEOUS METHOD (GREEN). *BOTTOM:* THE ESTIMATED ADDED MASS FOR THE FALLING LIFEBOAT AS A FUNCTION OF TIME. THE CROSSING OF THE FREE SURFACE IS CLEARLY VISIBLE IN THE ADDED MASS.

is sensitive to this ratio, as the workload increases during the entry phase. The anticipative method (15)+(16), however, remains efficient regardless of the added-mass ratio, as the boundary condition inside the wave simulation predicts the boat motion. The workload is reduced by a factor around 10 for the complete simulation.

4.2 Moored TLP

The second test case is a tension-leg platform in a long-crested wave. The platform is modelled as a rigid body with elastic mooring lines. It can perform large but finite translations and rotations in three dimensions, but it cannot deform or change in volume. The generalization of the algorithmic coupling method to deformable bodies will be presented in another paper at this conference [30].

The wave is a nonlinear 5th-order Stokes wave with a height

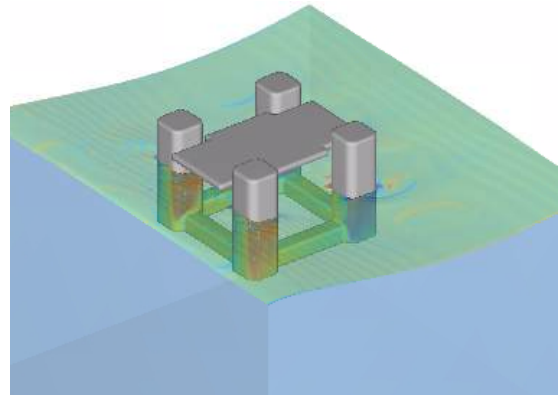


FIGURE 6. A SNAPSHOT FROM THE SIMULATION OF A TENSION-LEG PLATFORM IN A STOKES-5 WAVE.

of 23 cm. Since the variations around the waterline are small compared to the size of the platform, the added-mass ratio is relatively constant. Even for this moderate added-mass ratio, however, the anticipative method outperforms the relaxation-based method by a factor 2.5 to 3.0.

5 CONCLUSIONS

The ComFLOW simulation method has been designed to simulate and study extreme waves and their impact on falling, floating and moored structures. In particular, in this paper the (physical and numerical) interaction between the dynamics of the structure and the oncoming wave field is investigated. The efficiency of the numerical coupling is largely determined by the added-mass ratio, which seriously affects the existing partitioned coupling schemes based on the (sequential) exchange of loads and motions: a coupling with a higher range of added-mass ratios leads to loss of performance in these traditional coupling schemes. Inspired by developments in aerodynamic boundary-layer theory, an anticipatory, quasi-simultaneous coupling scheme has been developed which intends to circumvent most of the iterative coupling action. Application to two maritime applications, a free-fall life boat and a moored TLP, shows the new scheme to be robust and insensitive to the added-mass ratio. Whereas in the present paper the accent is on the behaviour of the numerical coupling algorithm, in future publications we will shift to the physical contents of the simulation results (including validation).

6 ACKNOWLEDGMENTS

This work is part of the research programme Maritime2013 with project number 13267 which is (partly) financed by the Netherlands Organisation for Scientific Research (NWO).

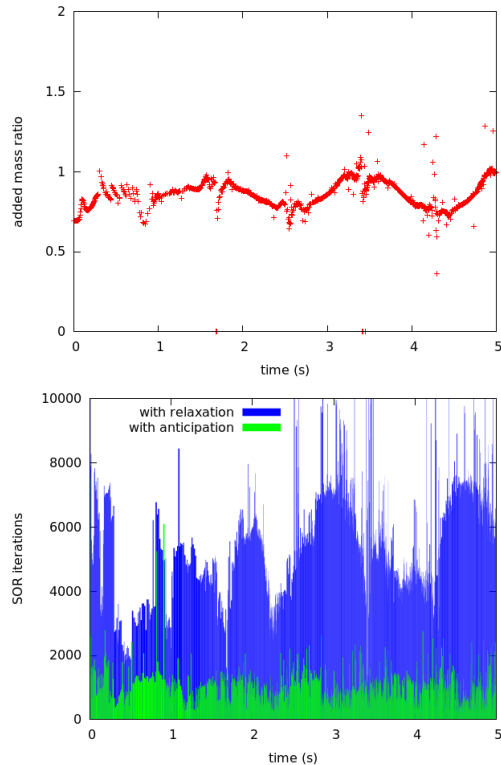


FIGURE 7. WORKLOAD OF THE SIMULATION OF A TENSION-LEG PLATFORM IN A STOKES-5 WAVE. *TOP:* VARIATION OF THE EFFECTIVE ADDED-MASS RATIO OVER TIME. *BOTTOM:* THE WORKLOAD FOR THE SIMULATION CORRESPONDS TO THE AREA UNDER THE CURVE.

REFERENCES

- [1] K.M.T. Kleefsman, G. Fekken, A.E.P. Veldman, B. Iwanowski, and B. Buchner. A Volume-of-Fluid based simulation method for wave impact problems. *J. Comput. Phys.*, 206:363–393, 2005.
- [2] A.E.P. Veldman, J. Gerrits, R. Luppés, J.A. Helder, and J.P.B. Vreeburg. The numerical simulation of liquid sloshing on board spacecraft. *J. Comput. Phys.*, 224:82–99, 2007.
- [3] A.E.P. Veldman, R. Luppés, T. Bunnik, R.H.M. Huijsmans, B. Düz, B. Iwanowski, R. Wemmenhove, M.J.A. Borsboom, P.R. Wellens, H.J.L. van der Heiden, and P. van der Plas. Extreme wave impact on offshore platforms and coastal constructions. In *30th Conf. on Ocean, Offshore and Arctic Eng. OMAE2011*, Rotterdam (Netherlands), June 19–24, 2011. Paper OMAE2011-49488.
- [4] A.E.P. Veldman, R. Luppés, H.J.L. van der Heiden, P. van der Plas, B. Düz, and R.H.M. Huijsmans. Turbulence modeling, local grid refinement and absorbing boundary conditions for free-surface flow simulations in offshore applications. In *Proc. 33rd Int. Conf. Ocean, Offshore and Arctic Eng.*, San Francisco (USA), June 8–13, 2014. OMAE2014-24427.
- [5] Rik Wemmenhove, Roel Luppés, Arthur E.P. Veldman, and Tim Bunnik. Numerical simulation of hydrodynamic wave loading by a compressible two-phase flow method. *Computers & Fluids*, 114:218–231, 2015.
- [6] B. Düz, R.H.M. Huijsmans, A.E.P. Veldman, M.J.A. Borsboom, and P.R. Wellens. An absorbing boundary condition for regular and irregular wave simulations. In L. Eça, E. Oñate, J. García-Espinosa, T. Kvamsdal, and P. Bergan, editors, *MARINE 2011, IV International Conference on Computational Methods in Marine Engineering, Selected Papers*, volume 29 of *Computational Methods in Applied Sciences*. Springer, 2013.
- [7] B. Düz. *Wave generation, propagation and absorption in CFD simulations of free surface flows*. PhD thesis, Technical University Delft, 2015.
- [8] B. Düz, M.J.A. Borsboom, A.E.P. Veldman, P.R. Wellens, and R.H.M. Huijsmans. The effect of different volume-of-fluid (VOF) methods on energy dissipation in simulations of propagating water waves. In preparation, 2017.
- [9] B. Düz, M.J.A. Borsboom, P.R. Wellens, A.E.P. Veldman, and R.H.M. Huijsmans. An absorbing boundary condition for free-surface water waves. *Comput. Fluids*, under revision, 2017.
- [10] R. Verstappen. When does eddy viscosity damp subfilter scales sufficiently? *J. Sci. Comput.*, 49(1):94–110, 2011.
- [11] W. Rozema. *Low-dissipation methods and models for the simulation of turbulent subsonic flow*. PhD thesis, University of Groningen, 2015.
- [12] W. Rozema, H.J. Bae, P. Moin, and R. Verstappen. Minimum-dissipation models for large-eddy simulation. *Phys. Fluids*, 27:085107, 2015.
- [13] P. van der Plas, A.E.P. Veldman, H.J.L. van der Heiden, and R. Luppés. Adaptive grid refinement for free-surface flow simulations in offshore applications. In *Proc. 34th Int. Conf. on Ocean, Offshore and Arctic Engineering OMAE2015*, St. John’s (Canada), 31 May–5 June, 2015. paper OMAE2015-42029.
- [14] P. van der Plas. *Local grid refinement for free-surface flow simulations*. PhD thesis, University of Groningen, 2017.
- [15] H.J.L. van der Heiden, A.E.P. Veldman, R. Luppés, P. van der Plas, J. Helder, and T. Bunnik. Turbulence modeling for free-surface flow simulations in offshore applications. In *Proc. 34th Int. Conf. on Ocean, Offshore and Arctic Engineering OMAE2015*, St. John’s (Canada), 31 May–5 June, 2015. paper OMAE2015-41078.
- [16] A.E.P. Veldman, R. Luppés, P. van der Plas, H.J.L. van der Heiden, J. Helder, and T. Bunnik. Turbulence modeling for locally-refined free-surface flow simulations in offshore applications. In *Proc. Int. Symp. Offshore and Polar Eng*

- ISOPE2015*, Kona (Hawaii, USA), 23-27 June, 2015. paper ISOPE2015-TPC-0282.
- [17] Mahdi Abkar, Hyun J. Bae, and Parviz Moin. Minimum-dissipation scalar transport model for large-eddy simulation of turbulent flows. *Physical Review Fluids*, 1(4):041701, 2016.
- [18] R.W.C.P. Verstappen and A.E.P. Veldman. Symmetry-preserving discretization of turbulent flow. *J. Comput. Phys.*, 187:343–368, 2003.
- [19] C.W. Hirt and B.D. Nichols. Volume of fluid (VOF) method for the dynamics of free boundaries. *J. Comput. Phys.*, 39:201–25, 1981.
- [20] A.E.P. Veldman. New, quasi-simultaneous method to calculate interacting boundary layers. *AIAA J.*, 19:79–85, 1981.
- [21] A.E.P. Veldman. Matched asymptotic expansions and the numerical treatment of viscous-inviscid interaction. *J. Eng. Math.*, 39:189–206, 2001.
- [22] A.E.P. Veldman. A simple interaction law for viscous-inviscid interaction. *J. Eng. Math.*, 65:367–383, 2009.
- [23] Mark Drela and Michael B. Giles. Viscous-inviscid analysis of transonic and low Reynolds number airfoils. *AIAA J.*, 25(10):1347–1355, 1987.
- [24] Jan Vierendeels, Lieve Lanoye, Joris Degroote, and Pascal Verdonck. Implicit coupling of partitioned fluid–structure interaction problems with reduced order models. *Computers & Structures*, 85(11):970–976, 2007.
- [25] Joris Degroote, Klaus-Jürgen Bathe, and Jan Vierendeels. Performance of a new partitioned procedure versus a monolithic procedure in fluid–structure interaction. *Computers & Structures*, 87(11):793–801, 2009.
- [26] A.E.J. Bogaers, S. Kok, B.D. Reddy, and T. Franz. Quasi-newton methods for implicit black-box fsi coupling. *Comput. Meth. Appl. Mech. Eng.*, 279:113–132, 2014.
- [27] David E. Keyes, Lois C. McInnes, Carol Woodward, William Gropp, Eric Myra, Michael Pernice, et al. Multiphysics simulations: Challenges and opportunities. *Int. J. High Perf. Comput. Appl.*, 27(1):4–83, 2013.
- [28] Arthur E.P. Veldman. ‘Missing’ boundary conditions? Discretize first, substitute next, and combine later. *SIAM J. Sci. Stat. Comput.*, 11(1):82–91, 1990.
- [29] E.F.F. Botta and M.H.M. Ellenbroek. A modified SOR method for the Poisson equation in unsteady free-surface flow calculations. *J. Comput. Phys.*, 60:119–134, 1985.
- [30] S.M. Hosseini Zahrae, A.E.P. Veldman, P.R. Wellens, I. Akkerman, and R.H.M. Huijsmans. The role of a structural mode shape-based interaction law to suppress added-mass instabilities in partitioned strongly-coupled elastic structure-fluid systems. In *Proc. 36th Int. Conf. on Ocean, Offshore and Arctic Engineering*, Trondheim (Norway), June 25–30, 2017. paper OMAE2017-62075.